

Effect of Organic Solvents and Electrode Materials on Electrochemical Reduction of Sulfur

Yongju Jung^{1,*}, Seok Kim², Bum-Soo Kim³, Dong-Hun Han⁴, Su-Moon Park⁴ and Juhyoun Kwak^{5,**}

¹ Nuclear Chemistry Research Division, Korea Atomic Energy Research Institute, P.O. Box 105, Yuseong, Daejeon 305-600, Korea

² Advanced Material Division, Korea Research Institute of Chemical Technology, P.O. Box 107, Yuseong, Daejeon 305-600, Korea

³ UP Chemical, 576-2 Chilgwe-Dong, Pyongtak-City, Kyunggi-Do 459-050, Korea

⁴ Department of Chemistry and Center for Integrated Molecular Systems, Pohang University of Science and Technology, Pohang, Gyeongbuk 790-784, Korea

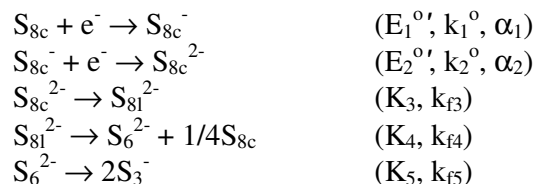
⁵ Department of Chemistry, Korea Advanced Institute of Science and Technology, 373-1 Guseong-dong Yuseong-gu, Daejeon 305-701, Korea

*E-mail: sonamu@kaeri.re.kr

**E-mail: jhkwak@kaist.ac.kr

Received: 12 December 2007 / Accepted: 25 February 2008 / Online published: 20 March 2008

The electrochemical reaction of sulfur has been studied through cyclic voltammetry (CV) method in six organic solvents including new solvent systems such as dimethoxyethane and diglyme. For the first time, the CV curves of sulfur are classified on the basis of the shape of the second reduction step. The overall shapes of CV curves, the peak potentials, and the potential shifts with scan rate were variable with the solvent used. These results apparently indicate that the solvent molecules are directly involved in the overall electrode reactions. Following reaction mechanism based on the successive one-electron reduction ($2 \times 1e^-$), which was proposed for the first redox waves of sulfur in our previous study, was verified both by digital simulation and by curve fitting to the CV curves obtained at glassy carbon (GC) and platinum (Pt) electrodes:



According to the mechanism, we obtained useful information such as formal potentials and standard rate constants from the first redox waves through digital simulation technique. The estimated standard rate constants (k_1^0 and k_2^0) of the two redox couples, *i.e.*, S_{8c}/S_{8c}^- and S_{8c}^-/S_{8c}^{2-} , at glassy carbon electrodes were much larger than those at platinum electrodes. We think this feature probably arose from the much higher affinities of sulfur to glassy carbon electrodes. Overall results indicate that the

electrode reactions of sulfur are significantly affected by the electrode material as well as the nature of solvent.

Keywords: Sulfur; Electrode materials; Organic Solvents; Electrochemical reduction; Digital simulation; Polysulfides; Cyclic voltammetry

1. INTRODUCTION

Lithium/sulfur (Li/S) batteries have been recently refocused as candidates for promising secondary batteries due to the high theoretical capacity of sulfur (1675 mAh/g) [1-9]. Electrochemical reduction of sulfur is known to be very complicated, and the reaction has been shown to be composed of a series of electron transfer reactions coupled with homogeneous chemical reactions [10-30]. The reduction products of sulfur, polysulfides S_n^{x-} ($n > 2$), dissolve in electrolytes to give a dark red or blue solution, which is dependent on solvent type. The characteristics of polysulfides such as reactivities, solubilities, etc. vary with the solvents [12-14,17,26,29]. This indicates that the performance of the positive electrode of Li/S batteries can be directly affected by the electrolyte systems. A number of investigators have studied the electrochemical reactions of sulfur in individual solvent. So far, dimethylformamide (DMF), dimethyl sulfoxide (DMSO), acetonitrile (AcN), tetrahydrofuran (THF) and dimethylacetamide (DMAc) were applied as such solvents. However, comprehensive overview on the influences of organic solvents on the electrochemical reduction of sulfur has not been presented. In the first part of this work, the electrochemical behaviors of sulfur in six organic solvents including new solvent systems such as dimethoxyethane and diglyme are presented for a deep understanding of the electrochemistry of sulfur, and further classified on the basis of the shape of the second reduction step for the first time. Recently, we reported on the overall picture of the reaction mechanism for sulfur reduction in DMF by an *in situ* spectroelectrochemical method [30]. We proposed two pathways, that is, the successive one-electron reduction ($2 \times 1e^-$) and the two-electron reduction ($1 \times 2e^-$) for the first redox waves of sulfur. In the second part of this work, the first redox waves of sulfur in DMF are reexamined to determine which of the two pathways (i.e., the $2 \times 1e^-$ and the $1 \times 2e^-$) is more suitable reaction mechanism. The proposed reaction mechanism for the first redox waves of sulfur is verified both by digital simulation and by curve fitting to the ohmic drop compensated CV curves obtained at glassy carbon and platinum electrodes. Furthermore, the effect of electrode material is quantitatively evaluated for the first time, according to the verified mechanism.

2. EXPERIMENTAL PART

Sulfur (Aldrich, 99.99%) was used as received. All solvents (battery grade) and supporting electrolytes (battery grade) were used as received from the Cheil Industries Inc. (Korea). The organic solvents studied were dimethoxyethane (DME), diglyme (DG), acetonitrile (AcN), dimethylformamide (DMF), dimethylacetamide (DMAc), and dimethyl sulfoxide (DMSO). The supporting electrolyte was either lithium trifluoromethanesulfonate ($LiCF_3SO_3$) or tetraethylammonium tetrafluoroborate

(TEABF₄). Handlings of the chemicals and all the measurements were carried out in an argon-filled glove box at room temperature to avoid any contamination of moisture and oxygen.

A conventional three-electrode system with one compartment cell was used for all the measurements, using glassy carbon (GC, 3.0 mm diameter) and platinum (Pt, 1.6 mm diameter) disk electrodes as working electrodes. These electrodes were polished with a 0.05 μm alumina solution prior to the electrochemical measurements. A platinum wire was used as a counter electrode and Li foil as a reference electrode.

For cyclic voltammetry and chronoamperometry experiments, Autolab potentiostat (PGSTAT 30) controlled with Ecochemie and Autolab GPES software was used. Ohmic drop compensation was applied in all the measurements. The chronoamperometric faradaic current was obtained from the total current subtracted by the non-faradaic current, which was recorded from the same electrolyte solution without sulfur under the same experimental conditions. The CV simulation and fitting to the experimental CV curves were performed with the digital simulation program developed by the KAIST electrochemistry group [31], which was coded on the basis of the Crank-Nicholson method [32] and the exponentially expanding space grid [33,34]. Curve fittings to experimental CV data were basically performed through nonlinear regression analysis based on the Levenberg-Marquardt method. Appropriate initial values of the parameters of which simulated curves approximate the experimental curves were chosen by trial and error, since initial values of some parameters such as potential, rate constant and transfer coefficient are very important in such curve fittings. So, then, curve fittings to experimental data were carried out and various reaction parameters were calculated.

3. RESULTS AND DISCUSSION

Fig. 1 shows a series of cyclic voltammograms (CVs) recorded for sulfur reduction in various solvents containing 1.0 M LiCF₃SO₃ at a glassy carbon electrode. Fig. 1A shows that the CVs recorded in DMF, in which two well-defined redox waves are observed, are very similar to those reported previously in the same solvent [22-26]. Upon increasing the scan rates from 100 mV/s to 1000 mV/s, two reduction peaks I and III shifted to more negative potential, and the first oxidation peak II shifted to more positive potential, while the second oxidation peak IV did not shift. Also, an anodic wave V at about 2.4 V is noticeable. We recently presented the overall picture of reaction mechanism for the sulfur reduction in DMF and identified the CV peaks [30].

The CVs showed quite different characteristics depending on the solvents used. One general feature was that the reversal peaks (peak IV) for the second reduction peak of III almost disappeared in the solvents such as DME, DG, and AcN whereas well-defined anodic peaks were observed in DMF, DMAc, and DMSO. In particular, the cathodic peak potentials were shifted significantly in a more negative direction in DME when compared with the corresponding peaks observed in DMF and the second reduction peak of III was significantly smaller than that in DMF. The potential shift observed for the second reduction with the increased scan rate was more pronounced in DME as well. We believe that the difference observed in different solvents arises from the characteristics of the electrode

reaction with the coupled chemical reactions that depend heavily on the solvent in view of the results from earlier works [12-14,17,22-26].

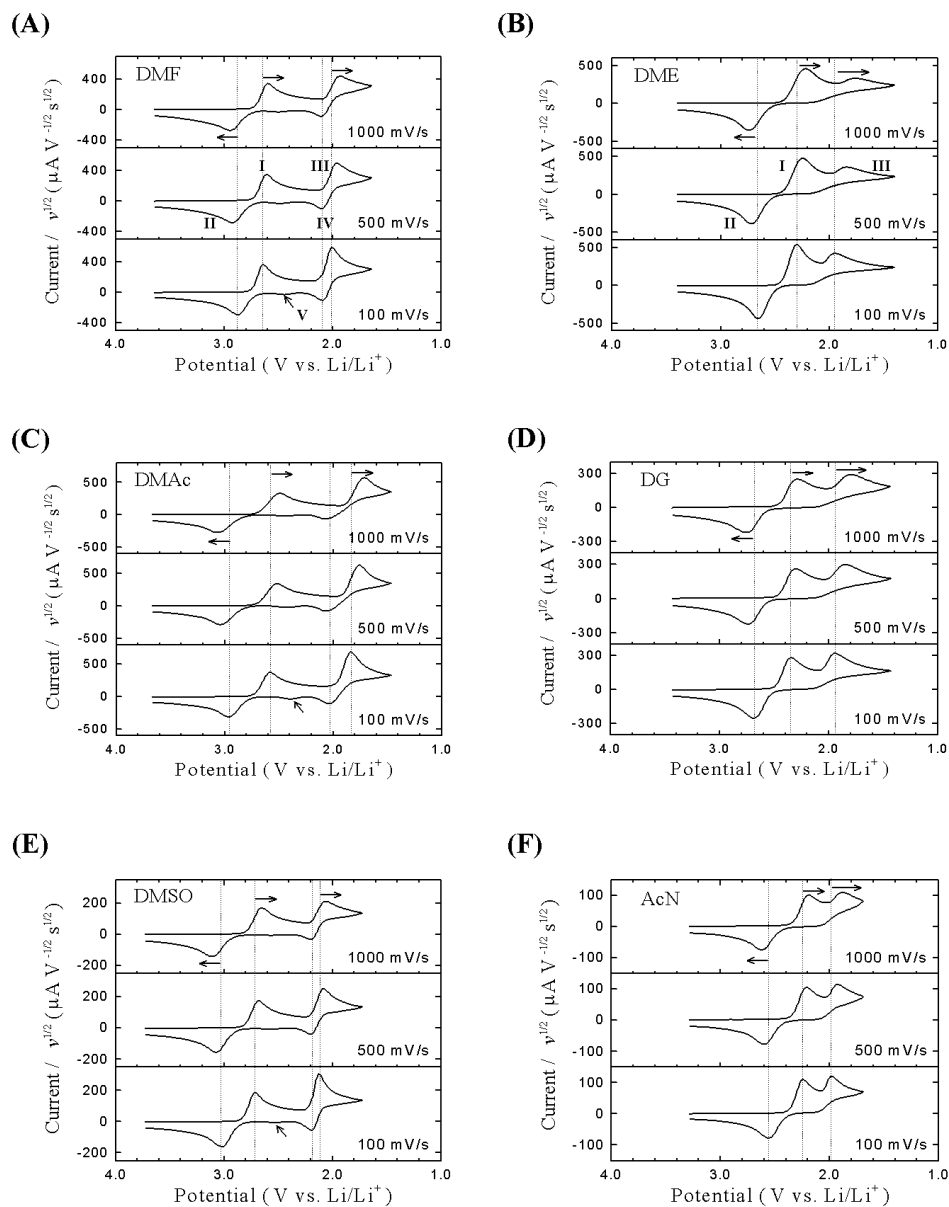


Figure 1. CV curves of sulfur in various organic solvents at glassy carbon electrodes (3.0 mm diameter): (A) 3.0 mM sulfur in DMF solution of 1M LiCF_3SO_3 ; (B) 4.0 mM sulfur in DME solution of 1M LiCF_3SO_3 ; (C) saturated sulfur in DMAc solution of 1M LiCF_3SO_3 ; (D) saturated sulfur in DG solution of 1M LiCF_3SO_3 ; (E) saturated sulfur in DMSO solution of 1M LiCF_3SO_3 ; (F) saturated sulfur in AcN solution of 1M LiCF_3SO_3 .

As pointed out, the CVs recorded in DMAc, DMF, and DMSO were in general very similar to each other. The same was true for the CVs observed in DME, DG, and AcN. The most important

solvent property that makes the sulfur reduction reactions so different appears to be its ability to solvate the primary reduction products. Fig. 2 shows two CV curves for the reduction of 3.0 mM S₈ in DMF when 1.0 M LiCF₃SO₃ (Fig. 2A) and 1.0 M TEABF₄ (Fig. 2B) were used as a supporting electrolyte. While the shapes of these curves are generally similar to each other, one notable feature is that the second reduction peak did not show potential shifts with increased scan rates when TEABF₄ was used. Also, the prewave was clearly observed at a low scan rate (100 mV/s) and at a higher potential than that of the second reduction peak III, which is similar to that reported elsewhere [23]. We conclude from these observations that the supporting electrolyte also influences the electrochemical reduction of sulfur.

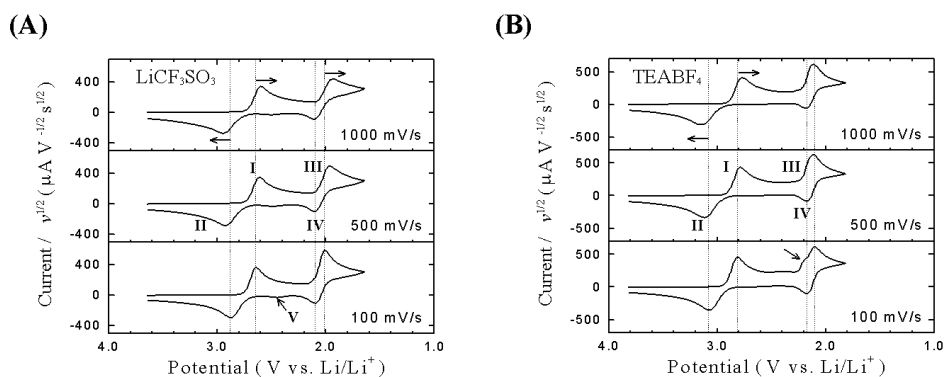
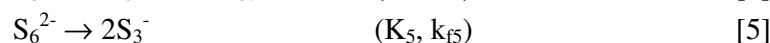
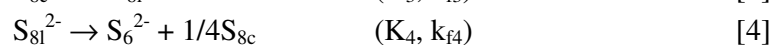
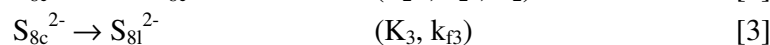
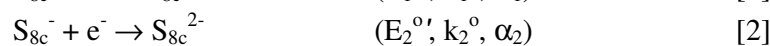
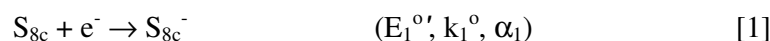


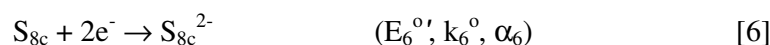
Figure 2. CV curves of sulfur in two DMF solutions with different supporting electrolytes at glassy carbon electrodes: (A) 3.0 mM sulfur in DMF solution of 1M LiCF₃SO₃ (the same as Fig. 1A); (B) 3.0 mM sulfur in DMF solution of 1M TEABF₄.

Summarizing the results of the CV studies, the overall shapes, the peak potentials, and the degree of the potential shifts with the scan rate were variable with various solvents and supporting electrolytes. We have observed at least three discretely different families of the shapes. These results apparently indicate that the solvent and supporting electrolyte are directly involved in the overall electrode reactions.

Recently, we reported on the overall picture of the reaction mechanism for sulfur reduction in DMF using an *in situ* spectroelectrochemical method [30]. In the case of the first redox wave, the following reaction mechanism was proposed:



or instead of [1] and [2]



Here, c and l in the subscripts denote the sulfur or the polysulfides with cyclic and linear structures, respectively.

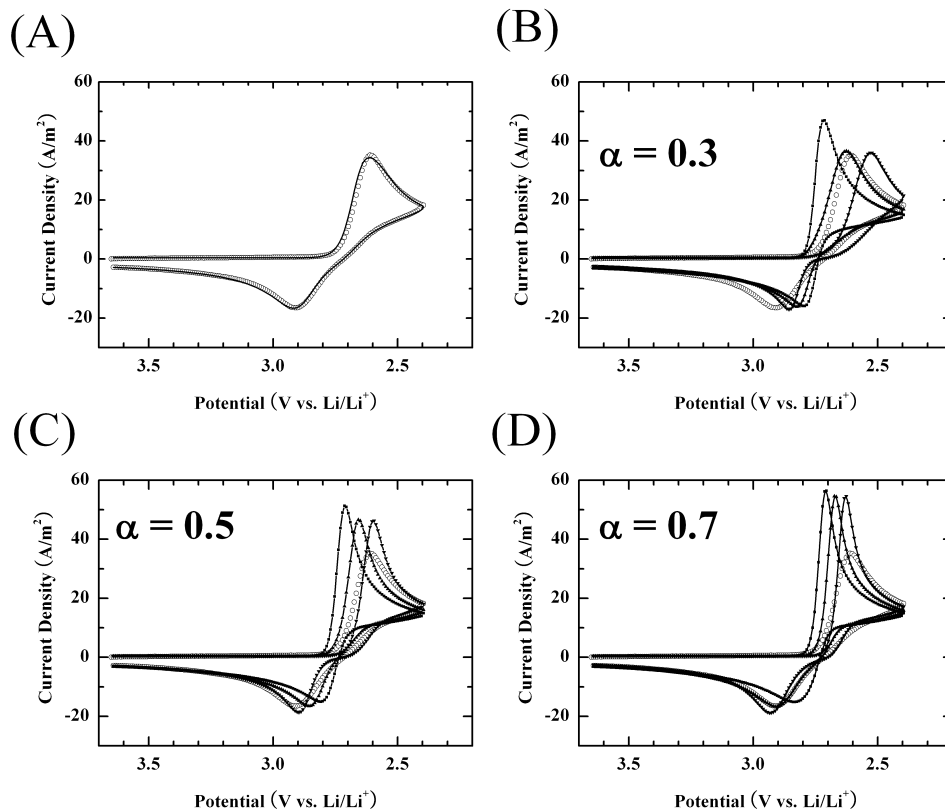


Figure 3. (A) Fitting of CVs (line) simulated according to the successive one-electron transfer-based mechanism (EECCC, equation [1] to [5]) to the experimental CVs (open circle) obtained in 3.0 mM sulfur in DMF solution of 1M LiCF_3SO_3 at glassy carbon electrodes and at the scan rate of 500 mV/s. Comparison of the same experimental CVs (open circle) with the fitted CVs (line + symbol) according to the two-electron transfer-based mechanism (ECCC, equation [3] to [6]) at various transfer coefficients (α) of 0.3 (B), 0.5 (C), and 0.7 (D) and at various standard rate constants of k^0 of 3.0×10^{-2} (■), 3.0×10^{-3} (▲), and 3.0×10^{-4} cm/s (▼).

In this study, we carried out a digital simulation to reveal which one of the two pathways, *i.e.*, the successive one-electron reduction ($2 \times 1e^-$) and the two-electron reduction ($1 \times 2e^-$), is more suitable reaction mechanism and then obtained the above physicochemical parameters from the mechanism showing the most satisfactory fits. Figures 3 and 4 show the CV data (open circle) for the reduction of 3 mM sulfur in DMF containing 1.0 M LiCF_3SO_3 at glassy carbon electrodes and at platinum electrodes, respectively. We can clearly see that the shapes of the CV curves were quite different from each other in two respects. First, the cathodic peak potential (E_{pc}) at platinum electrodes was observed in a much lower potential region than that at glassy carbon electrodes, and the anodic peak potential (E_{pa}) at platinum electrodes was observed in a much higher potential region than that at glassy carbon electrodes. As a result, the peak separation (ΔE_p) at platinum electrodes appeared much

larger than that at glassy carbon electrodes. It should be noted that ΔE_p at glassy carbon electrodes was also larger, compared with that of typical redox couple with reversible reaction. Second, the two experimental CV curves had basically asymmetrical shape with peak current ratio (i_{pa}/i_{pc}) less than 1.0 between the redox waves. However, the peak current ratio at platinum electrodes is much smaller when compared to that at glassy carbon electrodes. In addition, Fig. 3 shows a part of the digital simulation

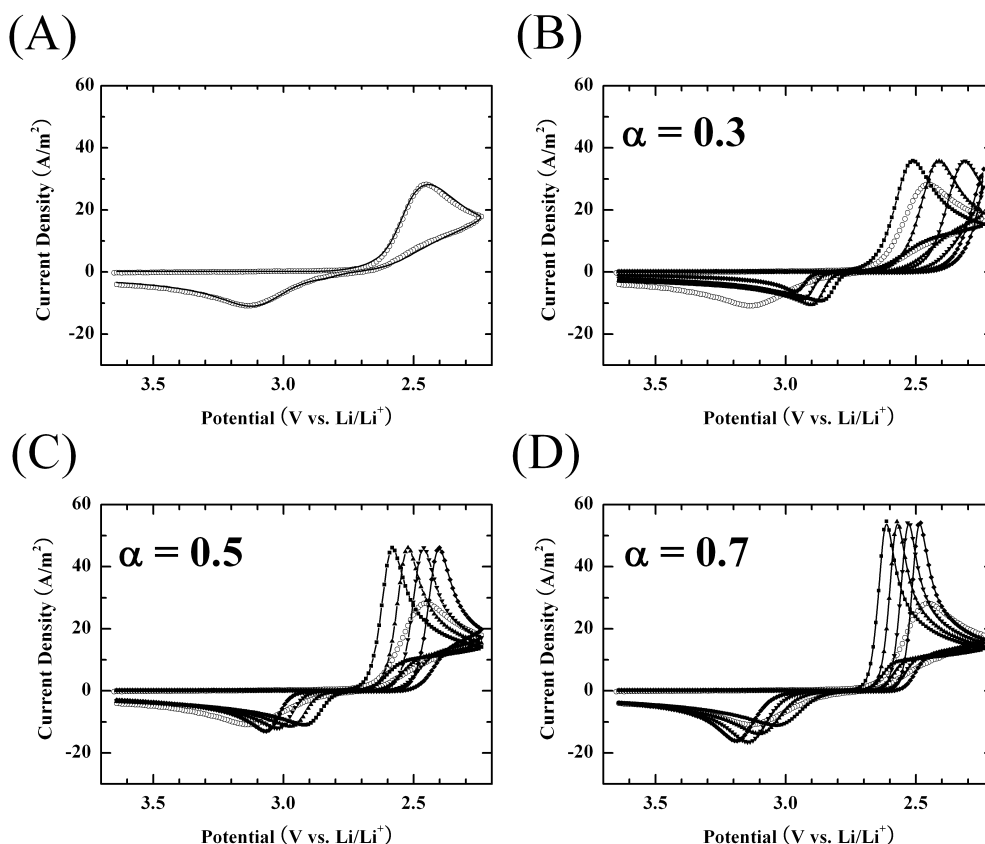


Figure 4. (A) Fitting of CVs (line) simulated according to the successive one-electron transfer-based mechanism (EECCC, equation [1] to [5]) to the experimental CVs (open circle) obtained in 3.0 mM sulfur in DMF solution of 1M LiCF_3SO_3 at platinum electrodes and at the scan rate of 500 mV/s. Comparison of the same experimental CVs (open circle) with the fitted CVs (line + symbol) according to the two-electron transfer-based mechanism (ECCC, equation [3] to [6]) at various transfer coefficients (α) of 0.3 (B), 0.5 (C), and 0.7 (D) and at various standard rate constants of k^0 of 3.0×10^{-4} (■), 3.0×10^{-5} (▲), 3.0×10^{-6} (▼), and 3.0×10^{-7} cm/s (□).

results for the first redox curves of sulfur at glassy carbon electrodes when scan rate was 500 mV/s. When the successive one-electron reduction ($2 \times 1e^-$) mechanism was applied, the simulated CV curve (line) showed an excellent fit to the experimental CV data (open circle) as shown in Fig. 3A. When the two-electron reduction ($1 \times 2e^-$) mechanism was applied, however, the simulated CV curves (line + symbol) showed poor fits to the experimental CV data (open circle) at wide transfer coefficients (α) range of 0.3 ~ 0.7 and at wide standard rate constants (k^0) range of 3.0×10^{-2} ~ 3.0×10^{-4} cm/s as shown

in Fig. 3B–3D. Fig. 4 shows a part of the digital simulation results for the first redox curves of sulfur at platinum electrodes when scan rate was 500 mV/s. We can clearly see that the CV curves (line + symbol) simulated by the two-electron reduction ($1 \times 2e^-$) mechanism are not adjusted to the experimental CV data (open circle) at all even under the various simulation conditions as shown in Fig. 4B–4D, unlike the simulation results (line) of the successive one-electron reduction ($2 \times 1e^-$) mechanism which showed excellent fits to the experimental CV data (open circle) at the scan rate of 500 mV/s as shown in Fig. 4A. Thus, we conclude that the $2 \times 1e^-$ is more confident pathway for the first waves of sulfur reduction than the $1 \times 2e^-$.

Furthermore, we performed a curve fitting to experimental CV curves to extract the following three kinds of parameters according to the successive one-electron reduction ($2 \times 1e^-$) mechanism (*i.e.*, equation [1] to [5]): i) the characteristic parameters for the electrode reaction such as $E^{o'}$ (formal potentials), k^o (standard rate constants), and α (transfer coefficients); ii) an average diffusion coefficient (D_s); and iii) the characteristic parameters for the homogeneous chemical reactions such as K (equilibrium constant) and k_f (homogeneous rate constants for forward reaction). Note that a curve fitting to experimental CV curves was carried out with the following assumptions: 1) diffusion coefficients of all sulfur species are identical as an average diffusion coefficient; 2) parameters related to the homogeneous chemical reaction are same both at Pt and at GC; 3) the formal potentials of electrode reactions are same both at Pt and at GC.

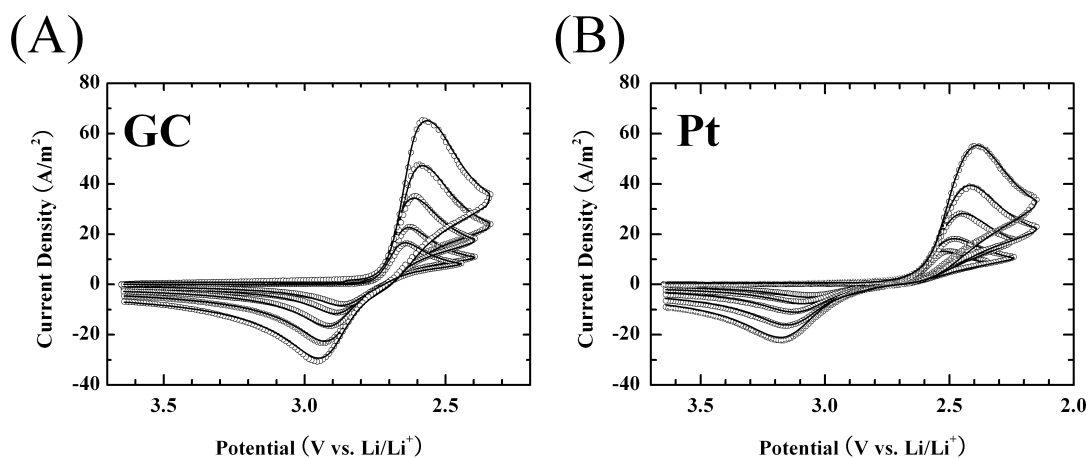


Figure 5. Comparison of the experimental CVs (open circles) with the simulated curves (lines) according to the successive one-electron transfer reduction ($2 \times 1e^-$) mechanism (EECCC) of equation [1] to [5] for the first redox waves at the five scan rates of 100, 200, 500, 1000 and 2000 mV/s: (A) 3.0 mM sulfur in DMF solution of 1M LiCF_3SO_3 at glassy carbon electrodes; (B) 3.0 mM sulfur in DMF solution of 1M LiCF_3SO_3 at platinum electrodes.

Fig. 5 shows a few examples of the simulated curves (line) fitted to the first redox waves of experimental CVs (open circle) obtained at five different scan rates (100, 200, 500, 1000 and 2000 mV/s) using glassy carbon or platinum electrodes. The simulation results showed excellent fits to all

the experimental CVs simultaneously at the two electrodes and at the five scan rates. The excellent fitting results strongly support the efficacy of the simulation technique as well as the validity of the reaction mechanism (equation [1] to [5]). Furthermore, they indicate that the disproportionation of S_{81}^{2-} (equation [4]) can not be ignored in the time scale of CV experiments at room temperature. Table 1 shows the various reaction parameters resolved by the simulation and curve fitting.

Table 1. Reaction parameters estimated from digital simulation and curve fitting method according to the successive one-electron transfer reduction ($2 \times 1e^-$) mechanism (EECCC) of equation [1] to [5] for the first redox waves of sulfur solution in DMF at glassy carbon electrodes (GC) and at platinum electrodes (Pt) with the following assumptions: 1) diffusion coefficients of all sulfur species are same; 2) parameters related to the homogeneous chemical reaction are same at the two electrodes; and 3) the formal potentials of electrode reactions are same at the two electrodes.

Electrode	$10^5 D_s$ (cm^2/s)	$S_{8c} + e^- \rightarrow S_{8c}^-$ [1]			$S_{8c}^- + e^- \rightarrow S_{8c}^{2-}$ [2]		
		$E_1^{o'}$ (V)	α_1	$\log(k_1^o)$ (cm/s)	$E_2^{o'}$ (V)	α_2	$\log(k_2^o)$ (cm/s)
GC	1.2	2.71	0.78	-2.42	2.71	0.46	-2.73
Pt			0.33	-3.18			
Electrode	K_3	$S_{8c}^{2-} \rightarrow S_{81}^{2-}$ [3]		$S_{81}^{2-} \rightarrow S_6^{2-} + 1/4S_{8c}$ [4]		$S_6^{2-} \rightarrow 2S_3^-$ [5]	
		$\log(k_{f3})$ (s^{-1})	K_4 ($M^{1/4}$)	$\log(k_{f4})$ (s^{-1})	K_5 (M)	$\log(k_{f5})$ (s^{-1})	
GC	3.76	3.51	0.002	-2.70	8.02	2.19	
Pt							

It was reported that the values of formal potentials of S_{8c}/S_{8c}^- (E_c) and S_{81}/S_{81}^{2-} (E_l) were -1.05 and -0.70 vs. Fc^+/Fc at 293 K, respectively, through a curve fitting based on ECE mechanism with assumption of $E_l > E_c$ [22]. In contrast, in this work, the values of formal potentials of the two redox couples (S_{8c}/S_{8c}^- and S_{8c}^-/S_{8c}^{2-}), i.e., $E_1^{o'}$ and $E_2^{o'}$, were unexpectedly found to be equal with the value of 2.71 V (vs. Li/Li^+). Note that reaction mechanisms of sulfur are quite different from each other. On the other hand, there was a large difference in the transfer coefficients (α_1 , α_2) and standard rate constants (k_1^o , k_2^o) between the two redox couples at the same electrode. The values of transfer coefficient ($\alpha_1 = 0.33$ and $\alpha_2 = 0.66$) at Pt were not surprising, as they were comparable with those ($\alpha_1 = 0.35$ and $\alpha_2 = 0.70$ at 293 K) reported elsewhere [22]. On the contrary, the values of transfer coefficient ($\alpha_1 = 0.78$ and $\alpha_2 = 0.46$) at GC were quite different from those at Pt. We think that this fact is caused by the affinity of reactant for electrode material. In general, hydrophobic elemental sulfur has higher affinity for glassy carbon electrodes than for platinum electrodes, and in contrast, polysulfide ions with a negative charge have higher affinity for platinum electrodes than for glassy carbon electrodes. For this reason, it is thought that α_1 has the value more than 0.5 and α_2 has the value less

than 0.5 at glassy carbon electrodes, while α_1 has the value less than 0.5 and α_2 has the value more than 0.5 at platinum electrodes. The standard rate constants for S_{8c}/S_{8c}^- were somewhat larger, compared with those for S_{8c}^-/S_{8c}^{2-} at GC and Pt. It is noteworthy that the standard rate constants (k_1^0 , k_2^0) at the glassy carbon electrodes were much larger than those at the platinum electrodes. We think this feature probably arose from the much larger affinities of sulfur to glassy carbon electrodes. This demonstrates clearly that the electrode materials as well as the solvents could affect the electrochemical reactions of sulfur significantly. The values of K_3 (3.76) and K_5 (8.02) mean that S_{8l}^{2-} and S_3^- are thermodynamically more stable species than S_{8c}^{2-} and S_6^{2-} , respectively. We have found a large discrepancy in the K_5 value (8.02 M) with that (0.073 M) reported earlier [23]. We think that the present result is much more credible considering the peak of S_3^- appeared stronger than that of S_6^{2-} in a thin-layer cell. Estimated value of the equilibrium constant (K_4) for the disproportionation of S_{8l}^{2-} was very similar to that ($0.002 M^{1/4}$) measured by the ESR study [21]. Table 1 also shows that the ring-opening of S_{8c}^{2-} and the dissociation of S_6^{2-} proceed very rapidly, but the disproportionation of S_{8l}^{2-} occurs slowly. The average diffusion coefficients of sulfur estimated from the simulation showed a good agreement with those calculated from the chronoamperometric current using the Cottrell equation [35]. The efficacy of the present simulation is confirmed well again from this agreement of the simulated values with the experimental values. Estimated value of the average diffusion coefficient at the glassy carbon electrodes was $1.2 \times 10^{-5} \text{ cm}^2/\text{s}$. The average diffusion coefficients of sulfur were relatively large in the solvents studied, compared with that of K^+ ($1.96 \times 10^{-5} \text{ cm}^2/\text{s}$ at 25 °C) in a dilute aqueous solution considering their respective sizes [36].

4. CONCLUSIONS

Overall shapes, peak potentials and the degree of the potential shifts with scan rate for the CVs of sulfur redox reaction depended largely on the solvents and supporting electrolytes. We have observed at least three discretely different families of the shapes. Type I that clearly shows second oxidation peak, was found in DMF, DMAc and DMSO solvents when Li salt was used as a supporting electrolyte. Type II that does not show second oxidation peak at all, was found in DME, DG, and AcN, when Li salt was used as a supporting electrolyte. Type III that shows reversible second step, was observed in DMF with TEABF₄ as a supporting electrolyte. Summarizing our results, the type I, type II and type III showed quasi-reversible, irreversible and reversible process in the second reduction step of elemental sulfur, respectively. Our results apparently indicate that both the solvent molecules and supporting electrolytes are directly involved in the overall electrode reactions.

Furthermore, the reaction mechanism based on the successive one-electron reduction ($2 \times 1e^-$), which was proposed for the first redox waves of sulfur in our previous study, was proved to be more suitable mechanism by digital simulation and by curve fitting to the CV curves obtained at glassy carbon and at platinum electrodes. According to the validated mechanism, we obtained useful information such as the formal potentials and standard rate constants from the first redox wave through digital simulation technique. Formal potentials of the two redox couples (i.e., S_{8c}/S_{8c}^- and S_{8c}^-/S_{8c}^{2-}) were unexpectedly found to be equal with the value of 2.71 V (vs. Li/Li⁺). On the other hand, there

was a large difference in the transfer coefficients and the standard rate constants between the two redox couples at the same electrode. The most noteworthy feature of the curve fitting results was that the standard rate constants of the two reductions at the glassy carbon electrodes were much larger than those at the platinum. We think this feature probably arose from the much higher affinities of sulfur to glassy carbon electrodes. Overall results indicate that the electrode reactions of sulfur are significantly affected by the electrode materials as well as the nature of solvents.

References

1. H. Yamin, A. Gorenshtein, J. Penciner, Y. Sternberg, E. Peled, *J. Electrochem. Soc.* 135 (1988) 1045.
2. E. Peled, Y. Sternberg, A. Gorenshtein, Y. Lavi, *J. Electrochem. Soc.* 136 (1989) 1621.
3. D. Marmorstein, T.H. Yu, K.A. Striebel, F.R. McLarnon, J. Hou, E.J. Cairns, *J. Power Sources* 89 (2000) 219.
4. B.H. Jeon, J.H. Yeon, K.M. Kim, I.J. Chung, *J. Power Sources* 109 (2002) 89.
5. S. Kim, Y. Jung, H.S. Lim, *Electrochim. Acta* 50 (2004) 889.
6. S. Kim, Y. Jung, S.J. Park, *J. Power Sources* 152 (2005) 272.
7. H.S. Ryu, H.J. Ahn, K.W. Kim, J.H. Ahn, J.Y. Lee, *J. Power Sources* 153 (2006) 360.
8. J.W. Choi, J.K. Kim, G. Cheruvally, J.H. Ahn, H.J. Ahn, K.W. Kim, *Electrochim. Acta* 52 (2007) 2075.
9. S. Kim, Y. Jung, S.J. Park, *Electrochim. Acta* 52 (2007) 2116.
10. M.V. Merritt, D.T. Sawyer, *Inorg. Chem.* 9 (1970) 211.
11. R.P. Martin, D.T. Sawyer, *Inorg. Chem.* 11 (1972) 2644..
12. T. Fujinaga, T. Kuwamoto, S. Okazaki, M. Hojo, *Bull. Chem. Soc. Jpn.* 53 (1980) 2851.
13. J. Paris, V. Plichon, *Electrochim. Acta* 12 (1981) 1823.
14. H. Yamin, J. Penciner, A. Gorenshtain, M. Elam, E. Peled, *J. Power Sources* 14 (1985) 129.
15. P. Dubois, J.P. Lelieur, G. Lepoutre, *Inorg. Chem.* 27 (1988) 73.
16. P. Dubois, J.P. Lelieur, G. Lepoutre, *Inorg. Chem.* 27 (1988) 1883.
17. B.S. Kim, S.M. Park, *J. Electrochem. Soc.* 140 (1993) 115.
18. G. Bossier, J. Paris, *New J. Chem.* 19 (1995) 391.
19. F. Gaillard, E. Levillain, *J. Electroanal. Chem.* 398 (1995) 77.
20. P. Leghie, E. Levillain, J.P. Lelieur, A. Lorriaux, *New J. Chem.* 20 (1996) 1121.
21. E. Levillain, P. Leghie, N. Gobeltz, J.P. Lelieur, *New J. Chem.* 21 (1997) 335.
22. E. Levillain, F. Gaillard, P. Leghie, A. Demortier, J.P. Lelieur, *J. Electroanal. Chem.* 420 (1997) 167.
23. F. Gaillard, E. Levillain, J.P. Lelieur, *J. Electroanal. Chem.* 432 (1997) 129.
24. E. Levillain, F. Gaillard, J.P. Lelieur, *J. Electroanal. Chem.* 440 (1997) 243.
25. A. Evans, M.I. Montenegro, D. Pletcher, *Electrochem. Commun.* 3 (2001) 514.
26. P. Leghie, J.P. Lelieur, E. Levillain, *Electrochem. Commun.* 4 (2002) 406.
27. P. Leghie, J.P. Lelieur, E. Levillain, *Electrochem. Commun.* 4 (2002) 628.
28. F. Scholz and C.J. Pickett (Eds.), *Encyclopedia of Electrochemistry*, vol. 7a, WILEY-VCH, Darmstadt, 2006 (Chapter 8).
29. R.D. Rauh, F.S. Shuker, J.M. Marston, S.B. Brummer, *J. Inorg. Nuc. Chem.* 39 (1977) 1761.
30. D.H. Han, B.S. Kim, S.J. Choi, Y. Jung, J. Kwak, S.M. Park, *J. Electrochem. Soc.* 151 (2004) E283.
31. F.R.F. Fan, J. Kwak, A.J. Bard, *J. Am. Chem. Soc.* 118 (1996) 9669.
32. K. Huebner, E.A. Thornton, *The Finite Element Method for Engineers*, John Wiley and Sons, Inc., New York, 1982.

33. T. Joslin, D. Pletcher, *J. Electroanal. Chem.* 49 (1974) 171.
34. S.W. Feldberg, *J. Electroanal. Chem.* 127 (1981) 1.
35. A.J. Bard, L.R. Faulkner, *Electrochemical Methods*, John Wiley and Sons, Inc., New York, 1980.
36. D.R. Lide, *CRC Handbook of Chemistry and Physics*, CRC Press, New York, 2000.